Numerical modelling of the swelling of clayey geomaterials by a multiscale approach

Hamza Mhamdi Alaoui
IC2MP Laboratory, University of Poitiers, Poitiers, France

Richard Giot
IC2MP Laboratory, University of Poitiers, Poitiers, France

Dimitri Prêt
IC2MP Laboratory, University of Poitiers, Poitiers, France

Philippe Cosenza
IC2MP Laboratory, University of Poitiers, Poitiers, France

Stephen Hedan
IC2MP Laboratory, University of Poitiers, Poitiers, France

ABSTRACT: The swelling of clay materials finds its origin at the different scales and is governed by two phenomena: crystalline and osmotic swelling. In this work, we propose a multi-scale numerical model that considers both swelling regimes. The model in its first version is based on a phenomenological approach to formulate the different interactions that occur in the interlayer space with respect to the disjoining pressure and the interparticular pores considering capillarity effects. The model is newly implemented in Code_Aster Finite Element software for hydro-mechanical coupling. The aim of this paper is to enhance the first model at its first implementation by adding: interparticular osmotic swelling along with the first existing aspect namely the capillarity effects at the interparticular pores scale. The validation of the updated model focuses on the swelling mechanism existing in constant-volume conditions in terms of swelling pressure. The model showed good accuracy compared to experimental results.

Keywords: Multi-scale modelling, Disjoining pressure, Homogenization, Osmotic swelling, Clay minerals.

1 THEORETICAL FORMULATION

The overall mathematical formulation given in Eq. (1) in tensorial notation, is based on the upscaling previously performed in Cariou et al. (2013). By means of Levin theorem, Cariou et al. (2013) upscaled the elasticity law from the clay layer level to the macro-scopic scale. The expression relates the macroscopic strain tensor ε_{kl} to the macroscopic stress tensor σ_{ij} using a new defined homogenized elasticity tensor C_{ijk}^{hom} and other parameters mainly the interparticular equivalent pressure P^{m}_{eq}, the disjoining pressure π_g, the liquid pressure p^l and that using the coupling parameters of Biot tensor b_i.

$$\sigma_{ij} = C_{ijkl}^{hom}.\varepsilon_{kl} - \left(\left(\delta p^l + \delta_n\, \pi_g\right)(1 - b_i) + \delta P_m^{eq} b_i\right) \qquad (1)$$

1.1 Elasticity parameters

The calculation of the different elasticity parameters through the elasticity tensor, are established using the Mori-Tanaka homogenization scheme that showed good accuracy on reproducing the elasticity parameters comparing to experimental measurements (Abou-Chakra Guéry et al. 2010). The mathematical formulation of the proposed scheme gives for the homogenized elasticity tensor:

$$C_{ijkl}^{hom} = C_{ijkl}^{mt,hom} + \frac{\varphi_{inc}}{1-\varphi_{inc}}(P_{ijkl})^{-1} \tag{2}$$

$$C_{ijkl}^{mt,hom} = (1-\varphi)C_{ijmn}^{iso,par}.\Big[(1-\varphi)I_{mnkl} + \varphi\big[I_{mnkl} - P_{mnop}.C_{opkl}^{iso,par}\big]^{-1}\Big]^{-1} \tag{3}$$

Eq. (2) gives the macroscopic homogenized elasticity tensor of the material whereas Eq. (3) formulates the homogenization scheme of the clay matrix of the material. Each tensor involved in Eq. (2-3) (i.e. P_{mnop}, $C^{iso,par}{}_{ijmn}$) is explained herein, P_{mnop} is the Hill tensor established for a spherical inclusion immerged in an isotropic matrix and $C^{iso,par}{}_{ijmn}$ the elasticity tensor of the clay particle with respect to the disjoining pressure; are calculated after conducting an isotropisation procedure (Bornert 2001). φ is the porosity within the interparticule pores, f is the nanoscopic porosity (porosity within the clay particle, mano-scale). I_{mnkl} is the fourth order identity tensor.

Similarly, we proceeded to formulate the coupling parameter Biot coefficient b_i it is also determined using an isotropization and Mori-Tanaka homogenization scheme:

$$b_i = \delta_{ij}.\left(I_{ijkl} - \left[C_{ijmn}^{iso,par}\right]^{-1}.C_{mnkl}^{hom}\right) \tag{4}$$

NB. The pore pressure is divided into two components interparticular pore pressure and the intraparticular pore pressure linked to each other through the thermodynamical equilibrium principle that reigns in the porous space of the clay matrix.

1.2 Disjoining pressure

This part of the mathematical formulation of the numerical model ticks off the different interactions existing in the interlayer space of the clay particle. It is based on a phenomenological approach used to itemize the different forces that reigns in the interlayer space. It is composed of the electrostatic forces formulated using Poisson-Boltzmann equation, responsible for the 4W (4 water layers accumulated in the interlayer space) hydration state of the interlayer osmotic swelling Eq. (6); the van-der-Walls molecular attraction force Eq. (8), the hydration forces: structural component also a repulsive constituent as the main mechanism accountable for the 1W-2W hydration states of crystalline swelling Eq. (9). The overall theoretical formulation of the disjoining pressure is given in Eqs. (8-13) where each parameter is detailed in Table 1. The disjoining pressure is therefore the sum of Eq (6) and Eq (8-9) (e.g., Gonçalvès et al, 2010). Using the convention of positive attractive forces.

$$\pi_g = \pi_d^{vdw} - \pi_d^e - \pi_d^s \tag{5}$$

$$\pi_d^e(h, c_i) = \frac{1}{CEC}\sum_{i\epsilon I} 2exc_i.c_i.N_A kT(cosh[u_i] - 1) \tag{6}$$

Table 1. Parameters of the disjoining pressure.

$\boldsymbol{I}$	Interlayer cations	$\boldsymbol{N_A}$	Avogadro number
$\boldsymbol{\varepsilon}$	Permittivity of the interlayer space	T	Temperature
$\boldsymbol{h}$	Interlayer spacing	k	Boltzmann constant
$\boldsymbol{exc_i}$	Exchangeable cation capacity	v_i	Cation valence
$\boldsymbol{CEC}$	Cation exchange capacity of the clay mineral	e'	Electronic charge
$\boldsymbol{c_i}$	Concentration of the cation in the interlayer space	S	Specific surface
$\boldsymbol{t}$	Thickness of the clay layer	A_h	Hamaker constant
$\boldsymbol{\kappa}$ $\boldsymbol{\lambda}$	Empirical parameters of the material		

$$u_i(h,c_i) = 8tanh^{-1}\left[exp\left[-\frac{h}{2}\sqrt{\frac{2c_iN_Av_i{}^2e'^2}{\epsilon kT}}\right] \times tanh\left[0{,}5sinh^{-1}\left[96{,}5\frac{exc_i}{S}\sqrt{\frac{1}{8\epsilon c_iN_AkT}}\right]\right]\right] \quad (7)$$

$$\pi_d^{vdw} = \frac{A_h}{24\pi}\left(\frac{1}{(h/2)^3} + \frac{1}{\left((h/2)+t\right)^3} - \frac{2}{\left((h/2)+(t/2)\right)^3}\right) \quad (8)$$

$$\pi_d^s = \kappa.\exp\left(\frac{-0.5h}{\lambda}\right) \quad (9)$$

1.3 Interparticular equivalent pressure

Interparticular pores within the clay matrix are difficult to characterize. Furthermore, due to the orientation of the clay particles, these last contributes to the complexity of the geometry of the porous space of the clay matrix. Besides, available techniques like mercury-porosimetry commonly considers the porous network as a set of cylinders or spheres. Considering that the porous space is henceforth constituted of two type of pores saturated either with water or air and both subjected to one pressure named equivalent pressure capturing capillarity effects and interfacial properties. Along with that, at this scale of the modelling, interparticular osmotic swelling that accounts for salinity effects also intervenes. Since the Poisson-Boltzmann equation fairly describes the double layer swelling it is also used there as the main function to formulate the osmotic pressure through p_π considering the chemical composition of the equilibrium solution within the interparticular pores. The formulation is weighted with the pore size distribution (PSD), and it is assumed that the PSD is better calibrated with Gaussian distributions. The threshold intervening in this part is calculated regarding the Laplace law applied between liquid and gaseous phase. The formulation reads:

$$P_m^{eq}(p_c) = \frac{1}{\chi}[\sum_i \int_{r_m}^{r^*} ((p^l + p_\pi) - \frac{2\gamma^{sl}}{r})\alpha^i(r)dr + \sum_i \int_{r^*}^{r_M} (p^g - \frac{2\gamma^{sg}}{r})\alpha^i(r)dr] \quad (10)$$

Where the interparticular osmotic pressure writes:

$$p_\pi(r, C_i) = \frac{1}{CEC} \sum_{i \epsilon E} 2EXC_i C_i N_A kT(cosh[u_i(r, C_i)] - 1) \quad (11)$$

Table 2. Terms of the interparticular equivalent pressure.

$\boldsymbol{\chi}$	Total volume of interparticular pores $\int_{r_m}^{r_M} \boldsymbol{\alpha(r)dr}$	$\boldsymbol{EXC_i}$	Exchange capacity of the cation within the interparticular space
$\boldsymbol{r_m}$-$\boldsymbol{r_M}$	Minimum and maximum pore radius respectively	C_i	Concentration of the cation within the interparticular space
$\boldsymbol{\alpha^i(r)}$	Pore size distribution (Gaussian distributions)	E	Cations within the equilibrium solution in the interparticular space
$\boldsymbol{p^l}$	Liquid pressure	p^g	Gas pressure
$\boldsymbol{\gamma^{sl}}$-$\boldsymbol{\gamma^{sg}}$	Surface tension solide-liquid, solid-gas respectively	r^*	Thresholding parameter $2\gamma^{lg}/p_c$

These assumptions allow us to define implicitly a new pivotal parameter capturing the water retention curve (WRC) of the material which links degree of saturation to the capillary pressure. It corresponds to the total volume of interparticular pores occupied with liquid divided by χ.

$$S_l(p_c) = \frac{1}{\chi} \int_{r_m}^{r^*} \alpha(r)dr \quad (12)$$

Once the formulation is achieved, the numerical model is then implemented in Code_Aster finite element method software for hydro-mechanical coupling. The model is implemented as a new definition of the effective stress that governs the chemo-hydromechanical behavior of clay geomaterials regarding the multi-scale formalism.

2 RESULTS AND DISCUSSIONS

The validation of the developed constitutive law lies in its ability to reproduce the well described swelling tests of clay materials available in the literature. To this aim, we focused on the swelling test of Callovo-Oxfordian argillite (hosting rock of radioactive wastes in France (ANDRA)) in constant-volume conditions (Zhang et al., 2020). Table 3 summarizes the cationic composition of the synthetic water equilibrium solution (WES) in Zhang et al., (2020). The calculation results are reported in Figure 1. The water is injected from the bottom at 0.01MPa occurring in 86.4s. The swelling pressure is measured at the upper face. The latter is calculated using the numerical model developed hereinbefore. The initial saturation degree is 90.46%.

Table 3. Cationic composition of the WES in ANDRA site of Bure.

Cation		Na^+	K^+	Ca^{2+}	Mg^{2+}
Concentration	[mol/m^3]	44.7	0.469	5.34	4.13
EXC	[mEq/g]	0.05	0.05	0.1	0.1

Table 4. Gaussian distributions parameters for different calculation tests.

Test	Parameter	Unit	Gaussian 1	Gaussian 2	Gaussian 3
Test 1	μ_i	[nm]	2	70	500
	σ_i	[nm]	0.5	5	10
	ω_i	[%]	35	15	50
Test 2	μ_i	[nm]	2	70	500
	σ_i	[nm]	0.5	40	240
	ω_i	[%]	35	15	50

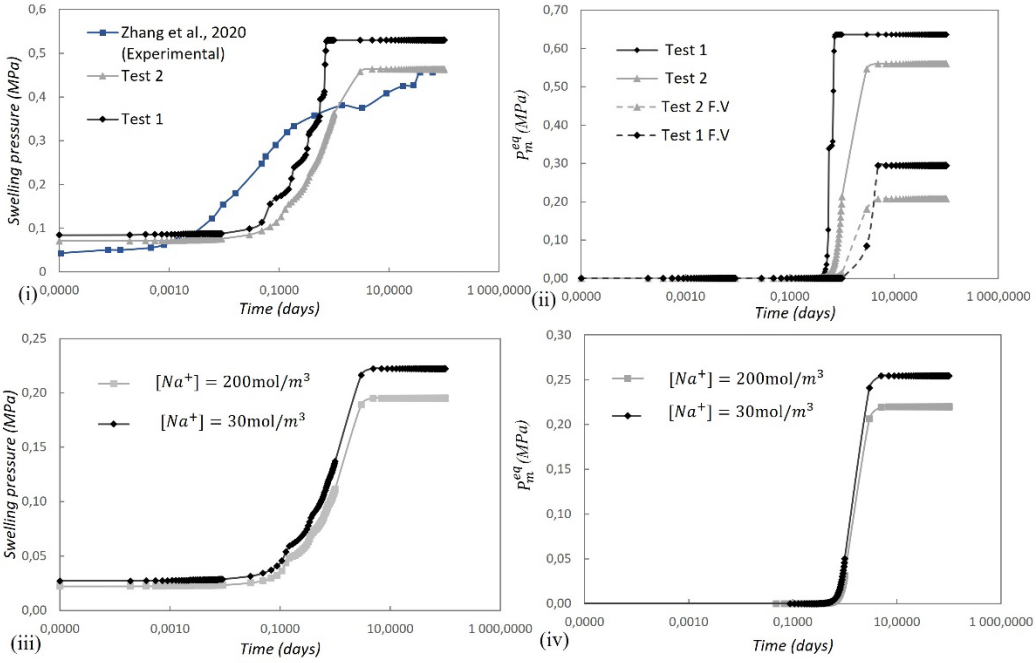

Figure 1. Calculation results. (i) Swelling pressure compared to experimental results in Zhang et al. (2020). (ii) Interparticular equivalent pressure where F.V stands for the first version of the model (no interparticular osmotic swelling considered). Effect of cationic concentration (calculation with only 1 cation) of WES on: (iii) Swelling pressure and (iv) Interparticular equivalent pressure.

The first noticeable result is that the model developed herein fairly reproduces the different kinematic phases of the swelling observed in constant-volume conditions, namely the initial swelling (first plateau); primary swelling (transient phase); secondary swelling (final plateau) that corresponds to the final measured swelling pressure.

Along with that, the PSD is a key parameter for complete modelling of the exact swelling behavior of the material. Enlarging the standard deviation smoothens the primary swelling phase besides, the stepwise saturation through the small sigmoids is no longer noticeable. The latter is only observed in Test 1 where narrow Gaussian distributions where considered, corresponding to throat of the pores generally exhibited through mercury-porosimetry techniques. Along with the kinematic observations, larger PSDs has also a significant role in improving the final swelling pressure. One can see that the final plateau is better fitted while using larger PSDs. Let us recall that the aim of the conducted tests in Zhang et al, (2020) is to measure the swelling pressure and that corresponds to the final plateau, secondary swelling phase.

Calculations in Figure 1(i-ii) where performed with respect to the real cationic concentrations in the WES of the Bure site (ANDRA) (see Table 3). Nevertheless, calculations for Figure 1(iii-iv) takes into account solely one cation: Na^+ with different concentrations. It is worth noting that the cationic concentrations are updated at each iteration during calculation with respect to the conservation law of molar quantity. The sensitivity analysis showed that increasing $[Na^+]$ tends to

reduce the swelling potential of the sample, this is consistent with the double-layer theory. This trend is directly linked to the equivalent interparticular pressure through the osmotic term detailed hereinbefore (Eq. (11)). Similar trend is also observed in experimental swelling tests for different chemical gradients (Rao and Thyagaraj, 2011)

3 CONCLUSION AND PROSPECTS

To conclude, the developed model considers the major aspects that chiefly reigns in the porous space of the clay material at both the nanoscopic scale through the disjoining pressure and the interparticular space with respect to capillarity, interfacial effects and double-layer swelling. That being said, a precise knowledge of all the different parameters will directly enhance the modelling for better results that will describe with good accuracy the swelling behavior. Mainly, the real PSD of the material considering a robust characterization of the PSD (Matskova et al., 2017).

Regarding literature, this new model accounts, for the first time, for both crystalline swelling at the nanoscale, interparticular osmotic swelling and capillarity effects occurring at the interparticular pores scale. The newly developed constitutive law is, indeed, completer and more pertinent for modelling major problematics in geomechanics (i.e., shallow foundations (<1.5-2m of depth) on clayey soils and also self-sealing of clayey rocks).

ACKNOWLEDGEMENTS

This work has been financially supported by the Région Nouvelle Aquitaine and Université de Poitiers. This work pertains to the French government program "Investissements d'Avenir" (EUR INTREE, reference ANR-18-EURE-0010). The work has also benefited from funding from the European Joint Program on Radioactive Waste Management EURAD-WP GAS (under grant agreement No 847593).

REFERENCES

Abou-Chakra Guéry, A., Cormery, F., Shao, J.-F., Kondo, D., 2010. A comparative micromechanical analysis of the effective properties of a geomaterial: Effect of mineralogical compositions. Comput. Geotech. 37, 585–593. https://doi.org/10.1016/j.compgeo.2010.02.008

Bornert, M., Bretheau, T., Gilormini, P., 2001. Homogénéisation en mécanique des matériaux, Tome 1 : Matériaux aléatoires élastiques et milieux périodiques. Hermes science.

Cariou, S., Dormieux, L., Skoczylas, F., 2013. An original constitutive law for Callovo-Oxfordian argillite, a two-scale double-porosity material. Appl. Clay Sci. 80–81, 18–30. https://doi.org/10.1016/j.clay.2013.05.003

Gonçalvès, J., Rousseau-Gueutin, P., de Marsily, G., Cosenza, P., Violette, S., 2010. What is the significance of pore pressure in a saturated shale layer? Water Resour. Res. 46.

Matskova, N., Prêt, D., Gaboreau, S., Cosenza, P., Brechon, R., Gener, I., Fialips, C. i., Dubes, G., Gelin, F., 2017. Towards a Balance of Pore Size Distribution of Unconventional Hydrocarbons Reservoirs: Combination of Bulk Techniques Applied on Comparable Sub-Samples Localized by 3-D X-ray µTomography, in: Unconventional Resources Technology Conference, Austin, Texas, 24-26 July 2017, SEG Global Meeting Abstracts. Society of Exploration Geophysicists, American Association of Petroleum Geologists, Society of Petroleum Engineers, pp. 2393–2410. https://doi.org/10.15530/urtec-2017-2689299

Rao, S.M., Thyagaraj, T., 2011, Swell-compression behaviour of compacted clays under chemical gradients. Canadian Geotechnical Journal, 44(5), 520-532. https:/doi.org/10.1139/t07-002

Zhang, F., Cui, Y.-J., Conil, N., Talandier, J., 2020. Assessment of Swelling Pressure Determination Methods with Intact Callovo-Oxfordian Claystone. Rock Mech. Rock Eng. 53, 1879–1888. https://doi.org/10.1007/s00603-019-02016-y